PROCEEDINGS OF SPIE

Applications of Digital Image Processing XLIII

Andrew G. Tescher
Touradj Ebrahimi
Editors

24 August – 4 September 2020
Online Only, United States

Sponsored and Published by
SPIE

Volume 11510

Part One of Two Parts

Proceedings of SPIE 0277-786X, V. 11510

Applications of Digital Image Processing XLIII, edited by Andrew G. Tescher,
Touradj Ebrahimi, Proc. of SPIE Vol. 11510, 1151001 · © 2020 SPIE
CCC code: 0277-786X/20/$21 · doi: 10.1117/12.2581642

The papers in this volume were part of the technical conference cited on the cover and title page. Papers were selected and subject to review by the editors and conference program committee. Some conference presentations may not be available for publication. Additional papers and presentation recordings may be available online in the SPIE Digital Library at SPIEDigitalLibrary.org.

The papers reflect the work and thoughts of the authors and are published herein as submitted. The publisher is not responsible for the validity of the information or for any outcomes resulting from reliance thereon.

Please use the following format to cite material from these proceedings:
Author(s), "Title of Paper," in *Applications of Digital Image Processing XLIII*, edited by Andrew G. Tescher, Touradj Ebrahimi, Proceedings of SPIE Vol. 11510 (SPIE, Bellingham, WA, 2020) Seven-digit Article CID Number.

ISSN: 0277-786X
ISSN: 1996-756X (electronic)

ISBN: 9781510638266
ISBN: 9781510638273 (electronic)

Published by
SPIE
P.O. Box 10, Bellingham, Washington 98227-0010 USA
Telephone +1 360 676 3290 (Pacific Time) · Fax +1 360 647 1445
SPIE.org

Printed in the United States of America by Curran Associates, Inc., under license from SPIE.

Publication of record for individual papers is online in the SPIE Digital Library.

SPIE. DIGITAL LIBRARY
SPIEDigitalLibrary.org

Paper Numbering: *Proceedings of SPIE* follow an e-First publication model. A unique citation identifier (CID) number is assigned to each article at the time of publication. Utilization of CIDs allows articles to be fully citable as soon as they are published online, and connects the same identifier to all online and print versions of the publication. SPIE uses a seven-digit CID article numbering system structured as follows:

- The first five digits correspond to the SPIE volume number.
- The last two digits indicate publication order within the volume using a Base 36 numbering system employing both numerals and letters. These two-number sets start with 00, 01, 02, 03, 04, 05, 06, 07, 08, 09, 0A, 0B … 0Z, followed by 10-1Z, 20-2Z, etc. The CID Number appears on each page of the manuscript.

Multichannel polarization sensing of polycrystalline blood films in the diagnosis of the causes of poisoning

Ivashkevich, Ya., Vanchulyak, O., Bachinsky, V., Ushenko, O., Gorsky, M., et al.

Ya. Ivashkevich, O. Vanchulyak, V. Bachinsky, O. Ushenko, M. Gorsky, V. Ushenko, O. Dubolazov, "Multichannel polarization sensing of polycrystalline blood films in the diagnosis of the causes of poisoning," Proc. SPIE 11510, Applications of Digital Image Processing XLIII, 115102R (21 August 2020); doi: 10.1117/12.2568445

SPIE.

Event: SPIE Optical Engineering + Applications, 2020, Online Only

Multichannel polarization sensing of polycrystalline blood films in the diagnosis of the causes of poisoning

Ya. Ivashkevich[1], O. Vanchulyak[1], V. Bachinsky[1], O.Ushenko[2], M.Gorsky[2], V.Ushenko[2], O. Dubolazov[2]

[1] Bukovinian State Medical University, 3 Theatral Sq., Chernivtsi, Ukraine, 58000
[2] Chernivtsi National University, 2 Kotsiubynskyi Str., Chernivtsi, Ukraine, 58012

a.dubolazov@chnu.edu.ua

ABSTRACT

The results of a study of the effectiveness in the differential diagnosis of cases of alcohol and carbon monoxide poisoning by azimuthally invariant polarizing Mueller-matrix microscopy are presented:

- multichannel sounding with differently polarized laser beams of histological sections of the brain, myocardium, adrenal glands, liver and polycrystalline blood films of the dead and multichannel polarization filtering of a series of microscopic images with algorithmic determination of coordinate distributions (maps):
    1. Muller-matrix invariants of linear birefringence of fibrillar networks (MMI LB);
    2. Mueller-matrix invariants of circular birefringence of optically active molecular complexes (MMI CB);
- statistical differentiation of MMI LB and MMI CB cards with the optically anisotropic component of histological sections of the brain, myocardium, adrenal glands, liver and polycrystalline blood films of the dead due to IHD (control group), alcohol poisoning (study group 1) and carbon monoxide (study group 2);
- determination of operational characteristics (sensitivity, specificity and balanced accuracy) of the strength of the multidimensional Mueller-matrix microscopy method for histological sections of the brain, myocardium, adrenal glands, liver and polycrystalline blood films of the dead of all groups.

Keywords: polarization, diagnosis, bood films.

1. MUELLER-MATRIX INVARIANTS AND THEIR RELATIONSHIPS WITH OPTICAL ANISOTROPY PARAMETERS

In section 1 of our work, we noted that numerous studies in the field of Mueller-matrix polarimetry of biological tissues and fluids[1-5] revealed the following most general symmetry of the matrix operator $\{F\}$ characterizing the optical anisotropy of a phase-inhomogeneous layer

$$\{F\} = f_{11}^{-1} \times \begin{Vmatrix} 1 & f_{12} & f_{13} & f_{14} \\ f_{21} & f_{22} & f_{23} & f_{24} \\ f_{31} & f_{32} & f_{33} & f_{34} \\ f_{41} & f_{42} & f_{43} & f_{44} \end{Vmatrix}. \quad (1)$$

Applications of Digital Image Processing XLIII, edited by Andrew G. Tescher, Touradj Ebrahimi, Proc. of SPIE Vol. 11510, 115102R · © 2020 SPIE
CCC code: 0277-786X/20/$21 · doi: 10.1117/12.2568445

Each of the elements f_{ik} of the Mueller-matrix operator (1) is integrally and ambiguously associated with various types of optical anisotropy (linear and circular birefringence and dichroism) of biological layers [6-8]. At the same time, 12 matrix elements change when the plane of the biological sample rotates around the axis of optical sensing. Therefore, there is an additional ambiguity in solving inverse problems

The functional and diagnostic capabilities of the Mueller-matrix mapping method can be expanded by using ?, in addition to four azimuthally independent matrix elements (MMI), there are a number of other angular invariants. Namely, linear combinations or superpositions of such elements, lengths of mathematical vectors, the parameters of which are formed by sets of elements of the Mueller matrix. In addition, the angles between such vectors turned out to be azimuthally invariant [9-11]:

• elements of the Mueller matrix

$$f_{11};\quad f_{14};\quad f_{41};\quad f_{44}. \tag{2}$$

• superposition of the elements of the Mueller matrix

$$\Phi_{22+33} = \left(f_{22} + f_{33}\right); \tag{3}$$

$$\Phi_{23-32} = \left(f_{23} - f_{32}\right). \tag{4}$$

• lengths of mathematical vectors

$$\begin{cases} V_{12+13} = \sqrt{f_{12}^2 + f_{13}^2}; \\ V_{21+31} = \sqrt{f_{21}^2 + f_{31}^2}; \\ V_{42+43} = \sqrt{f_{42}^2 + f_{43}^2}; \\ V_{24+34} = \sqrt{f_{24}^2 + f_{34}^2}; \end{cases}. \tag{5}$$

• angles

$$\cos\left(V_{42+43}, V_{24+34}\right) = \frac{-\sqrt{\left(f_{42}^2 + f_{43}^2\right)}}{\sqrt{\left(f_{24}^2 + f_{34}^2\right)}}. \tag{6}$$

$$\begin{cases} \left\{V_{12;13}\right\} = \dfrac{1}{\sqrt{f_{12}^2 + f_{13}^2}} \begin{pmatrix} f_{12}^2 - f_{13}^2 \\ 2 f_{12} f_{13} \end{pmatrix}; \\ \left\{V_{21;31}\right\} = \dfrac{1}{\sqrt{f_{21}^2 + f_{31}^2}} \begin{pmatrix} f_{21}^2 - f_{31}^2 \\ 2 f_{21} f_{31} \end{pmatrix}; \\ \left\{V_{42;43}\right\} = \dfrac{1}{\sqrt{f_{42}^2 + f_{43}^2}} \begin{pmatrix} f_{42}^2 - f_{43}^2 \\ 2 f_{42} f_{43} \end{pmatrix}; \\ \left\{V_{24;34}\right\} = \dfrac{1}{\sqrt{f_{24}^2 + f_{34}^2}} \begin{pmatrix} f_{24}^2 - f_{34}^2 \\ 2 f_{24} f_{34} \end{pmatrix} \end{cases}. \tag{7}$$

$$V_{22;33;23;32} = \sqrt{(f_{22} - f_{33})^2 + (f_{23} - f_{32})^2} \ . \qquad (8)$$

Thus, by using the MMI set (relation (2) - (8)), it is possible to expand the capabilities of Mueller-matrix mapping for statistical or screening laboratory studies of samples of biological layers (histological sections and polycrystalline films) of human organs in various problems of biomedical diagnostics.

However, the vast majority of tissue samples and human organ fluids are partially depolarizing. This circumstance necessitates the experimental or analytical detection of information on the optical anisotropy of biological layers against the background of the background of optical radiation depolarized by them. Therefore, it is relevant to search for new approaches to the principles of azimuthally invariant Muyller-matrix mapping by step-by-step (layer-by-layer) description of polarized radiation conversion processes by real partially depolarizing optically anisotropic structures of biological layers.

2. DIFFERENTIAL DIAGNOSIS OF ALCOHOL AND CARBON MONOXIDE POISONING BY STATISTICAL ANALYSIS OF THE MUELLER-MATRIX INVARIANT OF LINEAR BIREFRINGENCE OF HISTOLOGICAL SECTIONS OF THE BRAIN

In fig. 1 shows maps (fragments (1) - (3)) and histograms (fragments (4) - (6)) of the distribution of the MMI LB of histological brain sections from the study (fragments (1), (4)) and two control (fragments (2), (3), (5), (6)) groups of samples.

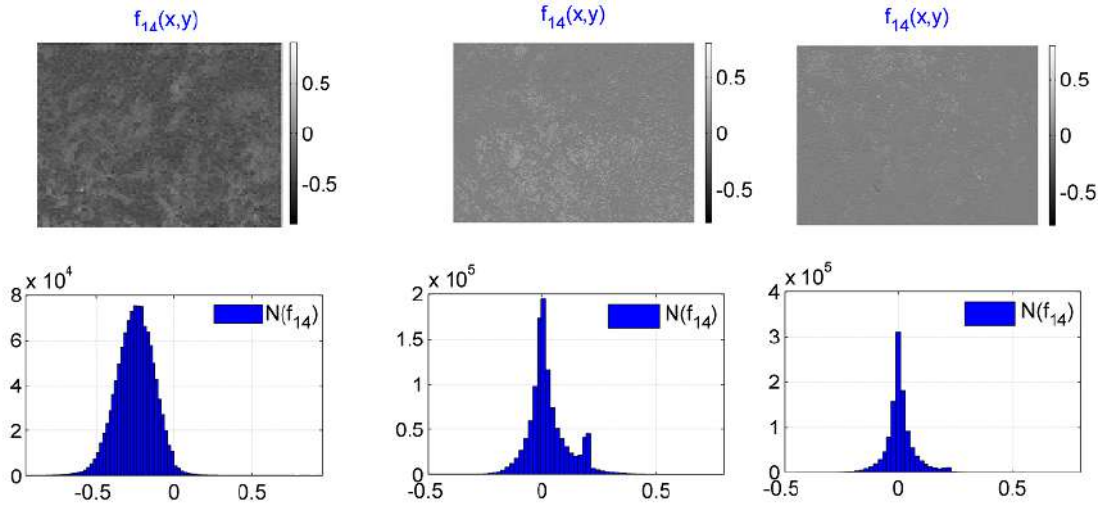

Fig. 1. Maps (fragments (1) - (3)) and histograms (fragments (4) - (6)) of the coordinate distributions of the MMI of the linear birefringence of histological sections of the brain of the dead from control group 1 (fragments (1), (4)), research group 2 (fragments (2), (5)) and research group 3 (fragments (3), (6)).

A comparative analysis of the coordinate distributions of the MMI CB value (fig. 1) revealed significant differences in the ranges of its change (fragments (4) - (6)) and the transformation of topographic structure (fragments (1) - (3)) of Mueller-matrix maps of histological sections of the brain of the dead from coronary heart disease and alcohol and carbon monoxide poisoning.

A tendency has been established to decrease the magnitude of statistical moments of the first and second orders, as well as an increase in the values of statistical moments of higher orders characterizing the asymmetry and excess (peak sharpness) of the histograms of the distribution of the MMI LB of brain samples of the dead as a result of poisoning with alcohol and carbon monoxide, - table 1.

Table 1. The central statistical moments of the 1st - 4th orders that characterize the coordinate distribution of the magnitude of the MMI LB of histological sections of the brain of the dead from the control and experimental groups

Sample	Histological sections of the brain		
Statistical moments	Group 1 ($n = 45$)	Group 2 ($n = 45$)	Group 3 ($n = 45$)
Average, *Sr*	$0{,}14 \pm 0{,}007$	$0{,}055 \pm 0{,}003$	$0{,}025 \pm 0{,}002$
$p_1; p_2$,		p_1 p 0,05	p_2 p 0,05
$p_{1;2}$		$p_{1;2}$ p 0,05	
Dispersion, *Dp*	$0{,}19 \pm 0{,}005$	$0{,}09 \pm 0{,}004$	$0{,}05 \pm 0{,}002$
$p_1; p_2$,		p_1 p 0,05	p_2 p 0,05
$p_{1;2}$		$p_{1;2}$ p 0,05	
Asymmetry, *As*	$0{,}36 \pm 0{,}014$	$0{,}71 \pm 0{,}034$	$1{,}23 \pm 0{,}059$
$p_1; p_2$,		p_1 p 0,05	p_2 p 0,05
$p_{1;2}$		$p_{1;2}$ p 0,05	
Excess, *Ek*	$1{,}36 \pm 0{,}061$	$1{,}07 \pm 0{,}052$	$0{,}86 \pm 0{,}042$
$p_1; p_2$,		p_1 p 0,05	p_2 p 0,05
$p_{1;2}$		$p_{1;2}$ p 0,05	

The statistical reliability ($p_1; p_2; p_{1;2}$ p 0,05) of the use in the differentiation of brain samples of deaths from all groups of the average *Sr* , dispersion *Dp* , asymmetry *As* and excesses *Ek* characterizing the distribution of the MMI LB in the differentiation of brain samples of the dead from the control group (IHD) and two experimental groups was established.

Using the principles of information analysis of the results of statistical processing of coordinate distributions of the values of MMI LB of histological sections of the brain, a satisfactory ($Sr, Dp \to 82\% - 83\%$) and good ($As, Ek \to 86\% - 88\%$) level of balanced accuracy in the differential diagnosis of cases of alcohol and carbon monoxide poisoning was found, - table 2.

Table 2. Operational characteristics of the strength of the Mueller-matrix polarimetry method

Sample	Histological sections of the brain							
$St_{i=1.2.3.4}$	Average, *Sr*		Dispersion, *Dp*		Asymmetry, *As*		Excess, *Ek*	
Se,%	a=38; b=7	84,4	a=37; b=8	82,2	a=39; b=6	86,6	a=40; b=5	88,8
Sp,%	c=37; d=8	82,2	c=37; d=8	82,2	c=38; d=7	84,4	c=39; d=6	86,6
Ac,%	n=45	83,3	n=45	82,2	n=45	85,5	n=45	87,7

3. DIFFERENTIAL DIAGNOSIS OF ALCOHOL AND CARBON MONOXIDE POISONING BY THE METHOD OF STATISTICAL ANALYSIS OF THE DISTRIBUTIONS OF THE MUELLER-MATRIX INVARIANT OF THE LINEAR BIREFRINGENCE OF HISTOLOGICAL SECTIONS OF THE MYOCARDIUM

The results of Mueller-matrix polarimetric mapping of histological sections of the myocardium from the research (fragments (1), (4)) and two control (fragments (2), (3), (5), (6)) groups are presented in a series of fragments of fig. 2.

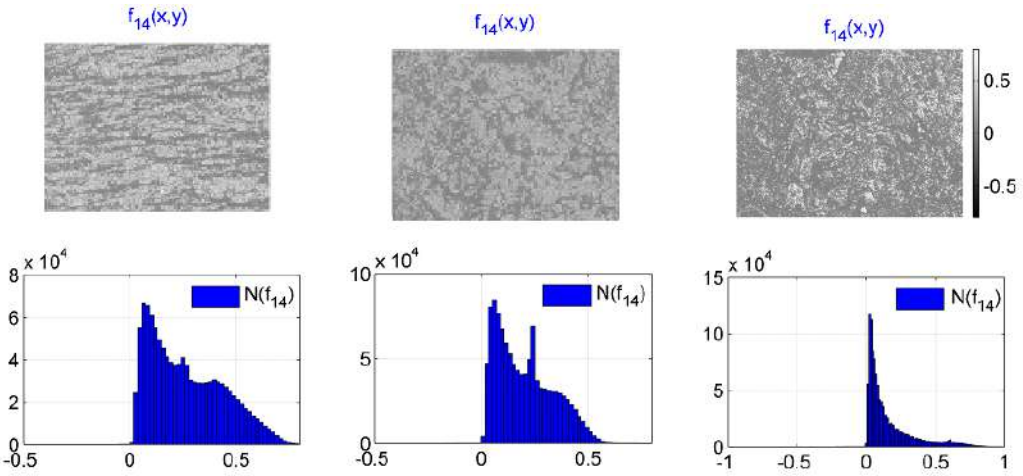

Fig. 2. Maps (fragments (1) - (3)) and histograms (fragments (4) - (6)) of the coordinate distributions of the MMI of the linear birefringence of histological sections of the myocardial deceased from control group 1 (fragments (1), (4)), research group 2 (fragments (2), (5)) and research group 3 (fragments (3), (6)).

As a result of Mueller-matrix polarization mapping of fibrillar myosin networks of myocardial samples (fig. 2), significant differences were revealed between the ranges of variations in the values of MMI LB (fragments (4) - (6)) and topographic structure (fragments (1) - (3)) experimentally measured MMI LB cards of samples of patients who died from coronary heart disease and alcohol and carbon monoxide poisoning.

Degenerative-dystrophic changes in myocardial tissue correspond to a decrease in the statistical moments of the 1st-2nd orders of magnitude (average and dispersion), as well as an increase in the statistical moments of the 3rd and 4th orders of magnitude characterizing the asymmetry and excess (peak sharpness) of the histograms of the distribution of magnitude MMI LB samples of histological sections of the myocardium of the groups of the dead as a result of poisoning by alcohol (research group 1) and carbon monoxide (research group 2) - table 3.

Table 3. The central statistical moments of the 1st - 4th orders, which characterize the coordinate distribution of the magnitude of the MMI LB of the histological sections of the myocardium of the dead from the control and experimental groups

Sample	Histological sections of the brain		
Statistical moments	Group 1 ($n = 45$)	Group 2 ($n = 45$)	Group 3 ($n = 45$)
Average, *Sr*	$0{,}28 \pm 0{,}013$	$0{,}17 \pm 0{,}008$	$0{,}08 \pm 0{,}004$
$p_1; p_2$,		p_1 p 0,05	p_2 p 0,05
$p_{1;2}$		$p_{1;2}$ p 0,05	
Dispersion, *Dp*	$0{,}39 \pm 0{,}017$	$0{,}21 \pm 0{,}011$	$0{,}095 \pm 0{,}005$
$p_1; p_2$,		p_1 p 0,05	p_2 p 0,05
$p_{1;2}$		$p_{1;2}$ p 0,05	
Asymmetry, *As*	$0{,}93 \pm 0{,}046$	$1{,}38 \pm 0{,}065$	$2{,}03 \pm 0{,}11$
$p_1; p_2$,		p_1 p 0,05	p_2 p 0,05
$p_{1;2}$		$p_{1;2}$ p 0,05	
Excess, *Ek*	$0{,}66 \pm 0{,}031$	$0{,}95 \pm 0{,}045$	$1{,}81 \pm 0{,}092$
$p_1; p_2$,		p_1 p 0,05	p_2 p 0,05
$p_{1;2}$		$p_{1;2}$ p 0,05	

A comparative analysis of the average (within representative samples of the sample) value of the set of central statistical moments of the 1st - 4th orders revealed the diagnostic effectiveness (statistical reliability $p_1; p_2; p_{1;2}$ p 0,05) of the method of azimuthally invariant Mueller-matrix microscopy in differentiating myocardial samples from all groups

Table 4 shows the results of determining the operational characteristics of the strength of the method of azimuthally invariant Mueller-matrix polarimetry of histological sections of the myocardium.

Table 4. Operational characteristics of the strength of the Mueller-matrix polarimetry method

Sample			Histological sections of the brain					
$St_{i=1.2.3.4}$	Average, *Sr*		Dispersion, *Dp*		Asymmetry, *As*		Excess, *Ek*	
Se,%	a=36; b=9	80	a=37; b=8	82,2	a=38; b=7	84.4	a=39; b=6	86,6
Sp,%	c=36; d=9	80	c=25; d=20	80	c=38; d=7	84,4	c=38; d=7	84,4
Ac,%	n=45	80	n=45	80,6	n=45	84,4	n=45	85,5

An information analysis of the results of statistical processing of the coordinate distributions of the magnitude of the MMI LB of histological sections of the myocardium showed a satisfactory ($Sr, Dp \to 81\%$) and good ($As, Ek \to 85\%$) level of balanced accuracy in the differential diagnosis of cases of alcohol and carbon monoxide poisoning

4. DIFFERENTIAL DIAGNOSIS OF ALCOHOL AND CARBON MONOXIDE POISONING BY STATISTICAL ANALYSIS OF THE MUELLER-MATRIX INVARIANT OF THE OPTICAL ACTIVITY OF HISTOLOGICAL SECTIONS OF THE BRAIN

On the fragments of fig. 3 shows topographic maps (fragments (1) - (3)) and histograms (fragments (4) - (6)) of the distributions of the magnitude of the MMI CB, which characterizes the optical activity of molecular complexes of histological sections of the brain with the research one (fragments (1), (4)) and two control (fragments (2), (3), (5), (6)) groups of samples.

Table 5 presents the data for determining the values of average values and errors (within each of the representative samples of the control and two research groups of samples of biological preparations) of a set of central statistical moments of the 1st - 4th orders of magnitude characterizing the average, dispersion, asymmetry and excess of distribution of the value MMI CB of histological sections of the brain of the dead.

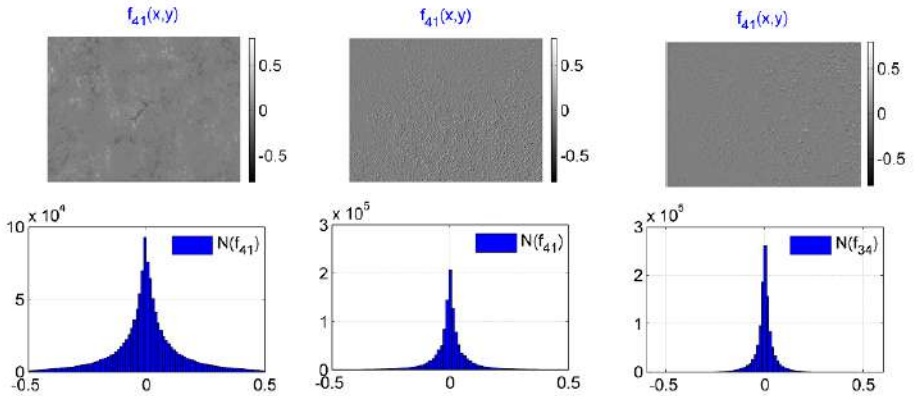

Fig. 3. Maps (fragments (1) - (3)) and histograms (fragments (4) - (6)) of the coordinate distributions of the MMI of the optical activity of the histological sections of the brain of the dead from control group 1 (fragments (1), (4)), research group 2 (fragments (2), (5)) and research group 3 (fragments (3), (6)).

It was found that the matrix parameter of the optical activity of histological sections of the brain decreases for cases of alcohol and carbon monoxide poisoning compared with coronary heart disease - the values of statistical moments of the first and second orders, asymmetry and excess of histograms of the distribution of the values of MMI CB are reduced, and vice versa they grow as a result of poisoning by alcohol and carbon monoxide gas - table 5.

The statistical uncertainty ($p_1; p_2; p_{1;2}$ f 0,05) of the use in the differentiation of samples of histological sections of the brain that died from all groups, the average distribution of the value of the parameter MMI CB of optically active molecular complexes.

For other statistical moments of the 2nd - 4th orders of magnitude, the differential diagnosis of cases of alcohol and carbon monoxide poisoning by statistical analysis of MMI CB maps of brain samples from both research groups is statistically significant – $p_1; p_2; p_{1;2}$ p 0,05 .

Table 5. The central statistical moments of the 1st - 4th orders that characterize the coordinate distribution of the magnitude of the MMI of circular birefringence of samples of histological sections of the brain of the dead from the control and experimental groups

Sample	Histological sections of the brain		
Statistical moments	Group 1 ($n = 45$)	Group 2 ($n = 45$)	Group 3 ($n = 45$)
Average, *Sr*	0,05 ± 0,003	0,04 ± 0,003	0,03 ± 0,002
$p_1; p_2$,		p_1 f 0,05	p_2 f 0,05
$p_{1;2}$		$p_{1;2}$ f 0,05	
Dispersion, *Dp*	0,125 ± 0,006	0,07 ± 0,004	0,06 ± 0,003
$p_1; p_2$,		p_1 p 0,05	p_2 p 0,05
$p_{1;2}$		$p_{1;2}$ f 0,05	
Asymmetry, *As*	0,63 ± 0,029	1,05 ± 0,052	1,73 ± 0,081
$p_1; p_2$,		p_1 p 0,05	p_2 p 0,05
$p_{1;2}$		$p_{1;2}$ p 0,05	
Excess, *Ek*	1,21 ± 0,059	2,07 ± 0,105	3,86 ± 0,14
$p_1; p_2$,		p_1 p 0,05	p_2 p 0,05
$p_{1;2}$		$p_{1;2}$ p 0,05	

Table 6. Operational characteristics of the strength of the Mueller-matrix polarimetry method

Sampe			Histological sections of the brain					
$St_{i=1.2.3.4}$	Average, *Sr*		Dispersion, *Dp*		Asymmetry, *As*		Excess, *Ek*	
Se,%	a=33; b=12	73,3	a=35; b=10	77,7	a=37; b=8	82,2	A=37; b=8	82,2
Sp,%	c=33; d=12	73,3	c=35; d=10	77,7	c=37; d=8	82,2	C=37; d=8	82,2
Ac,%	N=45	73,3	n=45	77,7	N=45	82,2	N=45	82,2

An information analysis of the results of statistical processing of the coordinate distributions of the MMI CB value found a satisfactory ($As, Ek \to 82\%$) level of balanced accuracy in the differential diagnosis of cases of alcohol and carbon monoxide poisoning.

5. DIFFERENTIAL DIAGNOSIS OF ALCOHOL AND CARBON MONOXIDE POISONING BY THE METHOD OF STATISTICAL ANALYSIS OF THE MUELLER-MATRIX INVARIANT OF THE OPTICAL ACTIVITY OF HISTOLOGICAL SECTIONS OF THE MYOCARDIUM

Fig. 4 illustrates the results of an azimuthally invariant Mueller-matrix polarimetric mapping of optically active molecular complexes of histological sections of the myocardial brain from the research (fragments (1), (4)) and two control (fragments (2), (3), (5), (6)) groups - coordinate (fragments (1) - (3)) and statistical (fragments (4) - (6)) distribution of MMI CB.

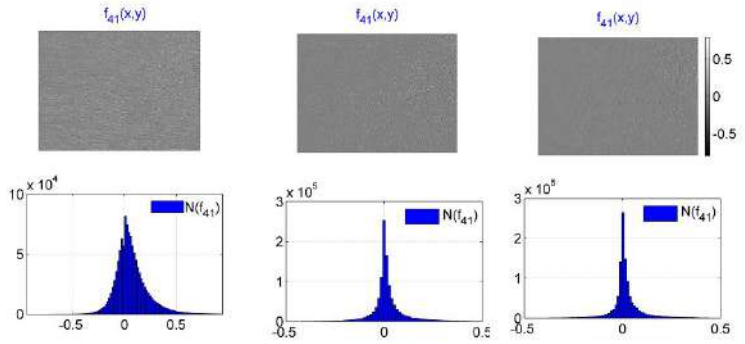

Fig. 4. Maps (fragments (1) - (3)) and histograms (fragments (4) - (6)) of the coordinate distributions of the MMI value of the optical activity of the histological sections of the myocardial deceased from control group 1 (fragments (1), (4)), research group 2 (fragments (2), (5)) and research group 3 (fragments (3), (6)).

As part of the statistical approach, it was found that degenerative-dystrophic changes in the optically active molecular complexes of myocardial tissue correspond to a decrease in the average and dispersion, as well as an increase in the asymmetry and excess of histograms of the distributions of the MMI CB values of the dead as a result of poisoning with alcohol and carbon monoxide, - table 7.

Table 7. The central statistical moments of the 1st - 4th orders that characterize the coordinate distribution of the MMI value of circular birefringence of samples of histological sections of the myocardium of the dead from the control and experimental groups

Sample	Histological sections of the brain		
Statistical moments	Group 1 ($n = 45$)	Group 2 ($n = 45$)	Group 3 ($n = 45$)
Average, *Sr*	0,07 ± 0,003	0,06 ± 0,003	0,045 ± 0,002
$p_1; p_2$,		p_1 f 0,05	p_2 f 0,05
$p_{1;2}$		$p_{1;2}$ f 0,05	
Dispersion, *Dp*	0,11 ± 0,005	0,07 ± 0,004	0,065 ± 0,003
$p_1; p_2$,		p_1 p 0,05	p_2 p 0,05
$p_{1;2}$		$p_{1;2}$ f 0,05	
Asymmetry, *As*	0,53 ± 0,023	0,91 ± 0,042	1,37 ± 0,063
$p_1; p_2$,		p_1 p 0,05	p_2 p 0,05
$p_{1;2}$		$p_{1;2}$ p 0,05	
Excess, *Ek*	0,88 ± 0,042	1,56 ± 0,077	2,71 ± 0,13
$p_1; p_2$,		p_1 p 0,05	p_2 p 0,05
$p_{1;2}$		$p_{1;2}$ p 0,05	

From the analysis of the magnitude of the central statistical moments of the 1st - 4th orders it follows:

- diagnostic unefficiency (statistical unreliability $p_1; p_2; p_{1;2}$ f 0,05) in the differentiation of myocardial samples from all groups of the deceased on the basis of calculating the average distribution of the magnitude of MMI CB;
- statistical reliability ($p_1; p_2$ p 0,05) of differentiation of myocardial samples of the dead from the control group (IHD) and two control groups by calculating the dispersion Dp ;
- diagnostic efficiency and statistical reliability ($p_1; p_2; p_{1;2}$ p 0,05) of differentiation of cases of alcohol and carbon monoxide poisoning based on the calculation of the asymmetry As and excess Ek values characterizing the distribution of the values of MMI CB.

The operational characteristics of the strength of the method of azimuthally invariant Mueller-matrix polarimetry of optically active molecular structures of histological sections of the myocardium are presented in table 8.

Table 8. Operational characteristics of the strength of the Mueller-matrix polarimetry method

Sampe			Histological sections of the brain					
$St_{i=1.2.3.4}$	Average, *Sr*		Dispersion, *Dp*		Asymmetry, *As*		Excess, *Ek*	
Se,%	a=33; b=12	73,3	a=33; b=12	73,3	a=35; b=10	77,7	A=35; b=10	77,7
Sp,%	c=33; d=12	73,3	c=33; d=12	73,3	c=34; d=11	75,5	C=34; d=11	75,5
Ac,%	N=45	73,3	n=45	73,3	N=45	76,6	N=45	76,6

An information analysis of the results of statistical processing of the coordinate distributions of the magnitude of the MMI CB revealed an unsatisfactory level (Ac π 80%) of balanced accuracy in the differential diagnosis of cases of alcohol and carbon monoxide poisoning.

5. DIAGNOSTIC EFFICIENCY OF THE MULTIDIMENSIONAL AZIMUTHALLY INVARIANT MUELLER-MATRIX POLARIMETRY METHOD

This section summarizes the results of an information analysis (the maximum level of balanced accuracy) of the diagnostic capabilities of objective digital forensic medical differentiation of cases of alcohol and carbon monoxide poisoning by multidimensional azimuthally invariant Mueller-matrix polarimetry of linear birefringence of fibrillar networks and circular birefringence of optically active molecular components of polycrystalline component of the histological sections of the brain, myocardium, adrenal glands, liver and polycrystalline films of the blood of the dead., - table 9 and table 10, respectively[13-15].

Table 9. The balanced accuracy of the method of multidimensional azimuthally invariant Muleler-matrix polarimetry of linear birefringence in the differentiation of cases of poisoning by alcohol and carbon monoxide

Biological layer	*Ac*,%	Level
Histological sections of the brain	**88**	Good
Histological sections of the myocardium	**85**	Good
Histological sections of the adrenal glands	**83**	Satisfactory
Histological sections of the liver	**80**	Satisfactory
Polycrystalline films of the blood	**83**	Satisfactory

Table 10. The balanced accuracy of the method of multidimensional azimuthally invariant Mueller-matrix polarimetry of circular birefringence in the differentiation of cases of poisoning by alcohol and carbon monoxide

Biological layer	*Ac*,%	Level
Histological sections of the brain	**82**	Satisfactory
Histological sections of the myocardium	**77**	Unsatisfactory
Histological sections of the adrenal glands	**86**	Good
Histological sections of the liver	**82**	Satisfactory
Polycrystalline films of the blood	**89**	Good

CONCLUSIONS

A comprehensive experimental study of the diagnostic effectiveness in differentiating cases of alcohol and carbon monoxide poisoning by a multi-parameter method of the azimuthally invariant Muller-matrix polarimetric microscopy of the linear and circular birefringent polycrystalline component of histological sections of the brain, myocardium, adrenal glands, and polycrystalline films of the blood of the dead.

A statistical differentiation of the coordinate distributions of the Mueller-matrix invariant of linear birefringence of fibrillar networks of histological sections of the brain, myocardium, adrenal glands, liver and polycrystalline blood films of the dead due to IHD (control group), alcohol poisoning (research group 1) and carbon monoxide (research group 2) was implemented .

The possibility of statistically significant ($p_1; p_2; p_{1;2}$ p 0,05) differentiation of cases of deaths from the control group (CHD) and cases of poisoning with alcohol and carbon monoxide by calculating the average *Sr* , dispersion *Dp* , asymmetry *As* and excess *Ek* , characterizing the distribution of the MMI LB of histological sections of the brain, myocardium, adrenal glands, liver and polycrystalline blood films was established.

The operational characteristics of the diagnostic strength of the method of Mueller-matrix polarimetry of the manifestations of linear birefringence were determined - sensitivity, specificity and balanced accuracy correspond to a satisfactory (adrenal gland, liver, blood) and good (brain, myocardium) level.

The possibility of statistically significant ($p_1; p_2; p_{1;2}$ p 0,05) differentiation of cases of deaths from the control group (IHD) and cases of poisoning with alcohol and carbon monoxide by calculating the dispersion *Dp* , asymmetry *As* and excess *Ek* , characterizing the distribution of the MMI CB of histological sections of the brain, myocardium, adrenal glands, liver and polycrystalline blood films was established.

The operational characteristics of the diagnostic strength of the method of Mueller-matrix polarimetry of the manifestations of circular birefringence of optically active molecular complexes were determined - sensitivity, specificity and balanced accuracy correspond to a satisfactory (brain, liver, myocardium) and good (adrenal glands, blood) level.

REFERENCES

[1]. Wang X. Propagation of polarized light in birefringent turbid media: a Monte Carlo study / X. Wang, L.-H. Wang // J. Biomed. Opt. – 2002. – Vol. 7. – P. 279-290.

[2]. Tuchin V. V. Handbook of optical biomedical diagnostics / V. V. Tuchin. – Bellingham : SPIE Press, 2002. – 1110 p.

[3]. Yao G. Two-dimensional depth-resolved Mueller matrix characterization of biological tissue by optical coherence tomography / G. Yao, L. V. Wang // Opt. Lett. – 1999. – V. 24. – P. 537-539.

[4]. Tower T. T. Alignment Maps of Tissues: I. Microscopic Elliptical Polarimetry / T. T. Tower, R. T. Tranquillo // Biophys. J. – 2001. – Vol. 81. – P. 2954-2963.

[5]. Lu S. Interpretation of Mueller matrices based on polar decomposition / S. Lu, R. A. Chipman // J. Opt. Soc. Am. A. –1996. – Vol. 13. – P.1106-1113.

[6]. Ghosh Nirmalya. Techniques for fast and sensitive measurements of two-dimensional birefringence distributions / Nirmalya Ghosh, I. Alex Vitkin // Journal of Biomedical Optics. – 2011. – № 16(11). – P. 110801.

[7]. Angelsky, O. V., Bekshaev, A. Y. A., Maksimyak, P. P., Maksimyak, A. P., & Hanson, S. G. (2018). Low-temperature laser-stimulated controllable generation of micro-bubbles in a water suspension of absorptive colloid particles. Optics Express, 26(11), 13995-14009.

[8]. Angelsky, O. V. (2007). Optical correlation techniques and applications. Optical correlation techniques and applications (pp. 1-270)

[9]. Angelsky, O. V., Ushenko, A. G., Pishak, V. P., Burkovets, D. N., Yermolenko, S. B., Pishak, O. V., & Ushenko, Y. A. (2000). Coherent introscopy of phase-inhomogeneous surfaces and layers. Paper presented at the Proceedings of SPIE - the International Society for Optical Engineering, 4016 413-418.

[10]. Angelsky OV, Bekshaev AY, Hanson SG, Zenkova CY, Mokhun II and Jun Z (2020) Structured Light: Ideas and Concepts. Front. Phys. 8:114.

[11]. Angelsky OV, Zenkova CY, Hanson SG and Zheng J (2020) Extraordinary Manifestation of Evanescent Wave in Biomedical Application. Front. Phys.

8:159.
[12]. Ushenko, Yu.A., Bachynsky, V.T., Vanchulyak, O.Ya., Dubolazov, A.V., Garazdyuk, M.S., Ushenko, V.A., "Jones-matrix mapping of complex degree of mutual anisotropy of birefringent protein networks during the differentiation of myocardium necrotic changes," (2016) Applied Optics, 55 (12), pp. B113-B119.
[13]. Ushenko, Yu.A., Dubolazov, A.V., Karachevtcev, A.O., Zabolotna, N.I., "A fractal and statistic analysis of Mueller-matrix images of phase inhomogeneous layers,"(2011) Proceedings of SPIE - The International Society for Optical Engineering, 8134, 81340P.
[14]. Ushenko, V.A., Dubolazov, A.V., "Correlation and self similarity structure of polycrystalline network biological layers Mueller matrices images," (2013) Proceedings of SPIE - The International Society for Optical Engineering, 8856.
[15]. "Cassidy, "Basic concepts of statistical analysis for surgical research," Journal of Surgical Research 128,199-206 (2005).